International Journal of Nanomedicine

Dovepress
open access to scientific and medical research

Open Access Full Text Article

ORIGINAL RESEARCH

Resveratrol-loaded solid lipid nanoparticles versus nanostructured lipid carriers: evaluation of antioxidant potential for dermal applications

This article was published in the following Dove Press journal:
International Journal of Nanomedicine
10 April 2012
Number of times this article has been viewed

Evren H Gokce[1]
Emrah Korkmaz[1]
Eleonora Dellera[2]
Giuseppina Sandri[2]
M Cristina Bonferoni[2]
Ozgen Ozer[1]

[1]Department of Pharmaceutical Technology, Faculty of Pharmacy, University of Ege, Izmir, Turkey; [2]Department of Drug Sciences, University of Pavia, Pavia, Italy

Background: Excessive generation of radical oxygen species (ROS) is a contributor to skin pathologies. Resveratrol (RSV) is a potent antioxidant. Solid lipid nanoparticles (SLN) and nanostructured lipid carriers (NLC) can ensure close contact and increase the amount of drug absorbed into the skin. In this study, RSV was loaded into SLN and NLC for dermal applications.

Methods: Nanoparticles were prepared by high shear homogenization using Compritol 888ATO, Myglyol, Poloxamer188, and Tween80. Particle size (PS), polydispersity index (PI), zeta potential (ZP), drug entrapment efficiency (EE), and production yield were determined. Differential scanning calorimetry (DSC) analysis and morphological transmission electron microscopy (TEM) examination were conducted. RSV concentration was optimized with cytotoxicity studies, and net intracellular accumulation of ROS was monitored with cytofluorimetry. The amount of RSV was determined from different layers of rat abdominal skin.

Results: PS of uniform RSV-SLN and RSV-NLC were determined as 287.2 nm ± 5.1 and 110.5 nm ± 1.3, respectively. ZP was −15.3 mV ± 0.4 and −13.8 mV ± 0.1 in the same order. The drug EE was 18% higher in NLC systems. TEM studies showed that the drug in the shell model was relevant for SLN, and that the melting point of the lipid in NLC was slightly lower. Concentrations below 50 μM were determined as suitable RSV concentrations for both SLN and NLC in cell culture studies. RSV-NLC showed less fluorescence, indicating less ROS production in cytofluorometric studies. Ex vivo skin studies revealed that NLC are more efficient in carrying RSV to the epidermis.

Conclusion: This study suggests that both of the lipid nanoparticles had antioxidant properties at a concentration of 50 μM. When the two systems were compared, NLC penetrated deeper into the skin. RSV-loaded NLC with smaller PS and higher drug loading appears to be superior to SLN for dermal applications.

Keywords: solid lipid nanoparticles, nanostructured lipid carriers, resveratrol

Introduction

Reactive oxygen species (ROS) are generated as by-products of cellular metabolism, primarily in mitochondria. When their production exceeds the cell's antioxidant capacity, macromolecules such as lipids, proteins, and DNA can be damaged.[1] Excessive generation of ROS in the skin is believed to be an important contributor to a variety of cutaneous pathologies, including different types of cancers.[2,3] ROS such as superoxide anion, hydrogen peroxide, and singlet oxygen, also play a critical role in many pathological conditions, including immune suppression, photo-aging, and photocarcinogenesis.[4–6] Using antioxidants as a therapeutic approach to overcome the occurrence of these pathologies appears promising.

Correspondence: Evren H Gokce
Ege University, Faculty of Pharmacy, 35100, Bornova, Izmir, Turkey
Tel +90232 3111368
Fax +90232 3885258
Email evrenhomangokce@gmail.com

Resveratrol (RSV) (trans-3,4,5-trihydroxystilbene), a phytoalexin found in grapes, nuts, fruits, and red wine, is a potent antioxidant with strong anti-inflammatory and antiproliferative properties.[7] RSV induces promyelocytic leukemia cell differentiation, and exhibits anticancer properties by mediating apoptosis, arresting cell cycle progression, antiproliferation and inhibiting ribonucleotide reductase, ornithine decarboxylase, and cyclooxygenase through modulation of prostaglandin production.[8]

Since their first description, solid lipid nanoparticles (SLNs) have attracted increasing attention as an efficient and nontoxic alternative lipophilic colloidal drug carrier, prepared either with physiological lipids or lipid molecules used as common pharmaceutical excipients. SLNs were developed in the early 1990s as an alternative carrier system to other colloidal formulations such as emulsions, liposomes, and polymeric nanoparticles. SLNs are produced by replacing the liquid lipid (oil) component of an oil/water emulsion with lipids that are solid at both room and body temperature.[9] In the second generation of lipid nanoparticle technology, the particles are produced using blends of solid lipids and oils – so-called nanostructured lipid carriers (NLCs).[10]

These lipid nanoparticles have many features that are advantageous for dermal application and can provide controlled release profiles.[11–13] They can be built from physiological and biodegradable lipids with generally recognized as safe (GRAS) status.[9,10] The irritant potential for skin and eyes as well as cytotoxicity for normal human keratinocytes is low.[14] The small size ensures close contact with the stratum corneum, and can increase the amount of drug absorbed by the skin. Lipid nanoparticles are also able to enhance the chemical stability of compounds sensitive to light, oxidation, and hydrolysis.[15–19]

The cellular uptake of RSV-loaded SLN and its beneficial effects on cellular fate has been evidenced recently in a cell culture study.[20] There does not, however, appear to be published comparative data available regarding the antioxidant effects of RSV-loaded SLNs and NLCs for dermal applications. The primary aim of this study was to design RSV-loaded SLNs and NLCs. The second aim was to evaluate the cytotoxicity and antioxidant capacity of SLNs and NLCs by determining the amount of ROS produced in fibroblasts, and the third aim was to evaluate the accumulation of RSV in different layers of skin.

Materials and methods

Materials

Compritol® 888 ATO (Glyceryl behenate) was generously supplied by Gattefossée (Nanterre, France). Poloxamer® 188 (Pluronic F68) was kindly donated by BASF (Ludwigshafen, Germany). Tween® 80 (Polysorbate 80) and RSV were obtained from Sigma Aldrich (Milan, Italy). Miglyol® 812 was purchased from Caelo (Hilden, Germany).

All high performance liquid chromatography (HPLC) reagents were purchased from Sigma Aldrich. The other chemicals were obtained from Carlo Erba (Milan, Italy). All filters were purchased from Sartorius AG (Milan, Italy).

Preparation of RSV-loaded SLNs and NLCs

RSV-loaded SLNs and NLCs were prepared by the high shear homogenization method.[21] The lipid phase – Compritol 888 ATO (C888) and 5 mg RSV – and the aqueous phase: 150 mg of Poloxamer 188 (P188) and 75 mg of Tween 80 (Tw 80) in 12.5 mL bidistilled water, were heated to 85°C, separately. The aqueous phase was poured into the lipid phase, at a stirring speed of 24,000 rpm with UltraTurrax (T25). The particles were dispersed in bidistilled water and kept at –20°C for 10 minutes. Blank SLNs were prepared in a similar way, without the drug. Different lipid-to-drug ratios have been studied to evaluate their effect on physical properties, as seen in Table 1. After determination of the optimum lipid-to-drug concentration, NLCs were prepared using the same method, by replacing 5%, 15%, 30%, and 45% of the solid lipid with liquid Miglyol oil.

Measurement of particle size and polydispersity index

Particle size (PS) and polydispersity index (PI) were measured at 25°C using Photon Correlation Spectroscopy

Table 1 The formulation parameters of produced SLNs and NLC

Code	The amount (mg) employed/25 mL of dispersion				
	C 888	Miglyol	P 188	Tw 80	RSV
S1	100	–	50	25	–
RS1	100	–	50	25	1
RS2	100	–	50	25	10
RS3	300	–	50	25	10
RS4	300	–	150	75	10
N1	285	15	150	75	–
N2	255	45	150	75	–
N3	210	90	150	75	–
N4	165	135	150	75	–
RN1	285	15	150	75	10
RN2	255	45	150	75	10
RN3	210	90	150	75	10
RN4	165	135	150	75	10

Abbreviations: NLC, nanostructured lipid carriers; RSV, resveratrol; SLNs, solid lipid nanoparticles; Tw, Tween.

(Zetasizer Nano ZS; Malvern, Milan, Italy) at an angle of 173° after dilution of formulations with bidistilled and filtered (0.45 μm) water. Each sample was measured in triplicate.

Measurement of zeta potential

The zeta potential (ZP) of SLN and NLC dispersions was measured at 25°C, under an electrical field of 40 V/cm (Zetasizer Nano ZS; Malvern). The measurements were conducted in triplicate.

Drug entrapment efficiency

In order to determine drug entrapment efficiency (EE), one end of the dialysis bag (cutoff 25 kDa) was tied, and the SLN or NLC dispersion was placed in the bag. The other opening of the bag was then closed. These bags were then placed in a centrifuge tube and the tube was filled with a mixture of ethanol and water (at a 1:1 ratio) and centrifuged for 1 hour at 14,000 rpm. The mixture of ethanol and water was then analyzed for RSV content by HPLC, allowing the quantity of free drug to be determined. The encapsulated amount of RSV was calculated by subtracting the free amount of RSV from the total amount present in the dispersion. Each batch was evaluated three times. The EE percentage was calculated by the following equation where *Wi* is the amount of initial drug and *Wf* is the amount of free drug:

$$EE\% = \frac{Wi - Wf}{Wi} \times 100 \quad (1)$$

The HPLC system (Agilent Series 1100; Data Apex, Milan, Italy) consists of a 25-cm long, 4-mm inner diameter stainless C18 column (ACE) and a mobile phase of methanol, water, and acetic acid (52:48:0.05 v/v/v). The flow rate and UV wavelength were set at 1 mL/min and 303 nm, respectively.

Lyophilization and the determination of production yield

Five milliliters of the SLN formulation was placed in 10 mL glass vials, without any cryoprotective agent. The samples were slowly frozen over 12 hours, and pre-cooled to –80°C. Lyophilization was performed at a pressure of 0.07 millibars for 24 hours at –45°C using a Christ Alpha 1-2 LD Freeze Dryer (Martin Christ Gefriertrocknungsanlagen GmbH, Hannover, Germany).

The production yield was calculated from the solid amount obtained from the lyophilization of SLNs, with the following equation:

$$Y\% = [(W_T - W_L)/W_T] \times 100 \quad (2)$$

where W_T is the theoretical amount and W_L is the lyophilizate amount.

Differential scanning calorimetry analysis

Differential scanning calorimetry (DSC) analysis was performed, with the samples sealed in aluminum pans under a nitrogen air atmosphere, at a flow rate of 20 mL/min and evaluated in 30°C–300°C temperature ranges (DSC 8000; Perkin Elmer, Milan, Italy). RSV, C 888, a physical mixture of C 888:RSV and SLN, and NLC formulation were evaluated.

Transmission electron microscopy (TEM) analysis

Morphological examination of the SLN and NLC was performed with a transmission electron microscope (CM12 Philips, Amsterdam, the Netherlands). The samples were stained with 2% (w/v) phosphotungstic acid and placed on copper grids for viewing by TEM.

Cell culture studies

Cytotoxicity studies

Normal Human Dermal Fibroblasts (NHDF) from juvenile foreskins (PromoCell GmbH, Heidelberg, Germany) were used. Cells between the 2nd and 5th passage were used for all experiments. Fibroblasts were grown in the presence of Dulbecco's modified Eagle medium (DMEM; Sigma) and supplemented with 10% fetal calf serum (FCS; Sigma) with 200 IU/mL penicillin, and with 0.2 mg/mL streptomycin and kept at 37°C in a 5% CO_2 atmosphere with 95% relative humidity.

Fibroblasts were seeded in each well of 96-well plates (area of 0.34 cm^2) at a density of 10^5 cells/cm^2. Cells were grown over 24 hours until their spatial arrangement was subconfluent. After 24 hours, the medium was replaced with a sample; in particular, the cells were put in contact with RSV-loaded SLN and NLC, and RSV alone at the following RSV concentrations: 10 μM, 25 μM, 50 μM, 100 μM, 250 μM, and 500 μM. Cell substrates were incubated for 24 hours. Subsequently, the medium was removed and the WST-1 (water soluble tetrazolium) test was performed. The WST-1 test is based on the activity of mitochondrial dehydrogenases of vital cells that convert WST-1 in a water soluble formazan. For this purpose, 100 μL of WST-1 solution (Roche Diagnostic, Milan, Italy) at 10% (v/v) in HBSS (Hank's Buffered Salt Solution) pH 7.4 was put in contact with each cell substrate for 3 hours. The absorbance of each well was assayed by means of an ELISA plate reader at 490 nm with

a reference of 655 nm.[22] Cell viability was calculated as a percentage ratio between the absorbance of each sample and the absorbance of complete growth medium.

Cytofluorimetry studies

To monitor net intracellular accumulation of ROS, the fluorescent probe DCFH-DA (2,7-dichlorfluoresceine acetate) was used. Fibroblasts were seeded in each well of a 12-well culture plate (with an area of 3.8 cm^2) at a density of 10^5 cells/cm^2. Cells were grown over 48 hours until their spatial arrangement was subconfluent, and were then put in contact with RSV-loaded SLN, RSV-loaded NLC, and RSV alone at 50 μM of RSV concentration. After 4 hours of contact, H_2O_2 at a concentration of 1.5 mM was added to each well. Cell substrates were then incubated for 24 hours. DCFH-DA at a concentration of 1 mM was put in contact with the cell substrates for 15 minutes.[23] Cells were then scraped from the bottom of each well and a cell suspension was obtained.

This suspension was then centrifuged at 1500 rpm for 5 minutes and the supernatant was removed. The cell pellet was then resuspended in 500 μL of phosphate buffered saline (PBS). Each cell suspension was assayed by means of a cytofluorimeter (Navios Flow Cytometer; Beckman Coulter, Inc, Milan, Italy) using an excitation wavelength of 488 nm, and the emission was then evaluated at a wavelength of 525 nm. The data collected were analyzed by means of Kaluza® Analysis software (v 1.2; Beckman Coulter, Inc). The results obtained for the cell substrates put in contact with H_2O_2 resulted in maximum oxidative damage (100%).

Ex vivo diffusion studies

Rat abdominal skin was excised immediately after the animal sacrifice, and purified from the surrounding tissue. The skin was placed in a Franz diffusion cell and 200 μL of the formulations was evaluated. The receptor phase consisted of ethanol and water at a ratio of 1:1 at 37°C and sink conditions were taken into consideration. The formulations to be tested were kept in contact with the tissue for 24 hours, and at certain time intervals, the RSV amount was determined in the samples taken from the receptor phase.

After 24 hours, the skin samples were taken, the excess formulation removed, and the skin surface cleaned with dry paper. The epidermis was separated from the dermis by means of heat application.[24] The tissue samples were homogenized using an Ultra-Turrax (IKA, Guangzhou, China) at 8000 rpm for 10 minutes (in 2 mL of ethanol) and the accumulated amount of RSV in the skin was extracted with the aid of a horizontal shaker for an additional 24 hours.

Statistical analysis

Statistical differences were determined using analysis of variance (ANOVA), followed by Tukey's test for comparisons between groups. The significance level was taken as 95% ($P < 0.05$).

Results and discussion

Preparation of RSV-loaded SLNs and NLCs

The particle size values were evaluated to understand the effect of the lipid-to-drug ratio on the physical properties of SLN as shown in Table 2.

It was observed that larger nanoparticles could be obtained with the increment of the RSV amount in the SLN formulations and the polydispersity indices detected were higher. This result was thought to be due to insufficient lipid to encapsulate the antioxidizing agent. When the amount of lipid was tripled, the SLN system returned to its homogenous form with a PI of 0.181. As with the lipid, when the surfactant concentrations were tripled, the particle dimensions were found to be smaller. In light of these studies, the optimum SLN formulation was determined as the RS4 with smaller particles in a uniform dispersion.

The ZP of S1 (the SLN formulation without any RSV added) was found to be −23 mV ± 0.8. However, the addition of RSV decreased the overall charge of the nanoparticles, and the ZP was then determined as −15.3 mV ± 0.4. The drug EE of RS4 was determined as 73% by a validated HPLC method. The production yield was 96%.

NLC formulations were prepared by taking RS4 as the starting formulation. Amounts of 5%, 15%, 30%, and 45% of the solid lipid were replaced with Miglyol oil in formulations coded as RN1, RN2, RN3, and RN4, respectively. Blank NLC formulations (N1, N2, N3, and N4) were also studied in terms of PS, PI, and ZP.

Surprisingly, the particle dimensions reduced when Miglyol was added to the system. The incremental amount of Miglyol directly affected the particle size. However, even in that case, the

Table 2 PS and PI of blank and RSV-loaded SLNs prepared

Code	PS (nm) ± SD	PI ± SD
S1	174.3 ± 1.8	0.229 ± 0.12
RS1	191.2 ± 3.9	0.580 ± 0.14
RS2	718.1 ± 8.9	0.664 ± 0.02
RS3	287.2 ± 5.1	0.181 ± 0.12
RS4	161.4 ± 2.7	0.263 ± 0.05

Note: Data are presented as mean ± standard deviation (SD).
Abbreviations: PI, polydispersity index; PS, particle size; RSV, resveratrol; SLNs, solid lipid nanoparticles.

size of NLCs was smaller than those of the SLNs in all of the oil-containing lipid concentrations. The presence or absence of RSV did not significantly affect the PS of N1, N2, and N3 formulations. However, the highest level of oil incorporation (45%) resulted in a greater PS when compared to blank NLCs.

This result can be explained by the emulsification of the system. In our previous study, the heating of the system was found to be very important during the melting and mixing of the solid lipid.[21] It was observed that the lipid base (C 888) had a tendency to return to solid form during mixing. C 888 is a mixture of mono-, di-, and triglycerides. It is well known that the longer the fatty acid triglyceride, the greater the energy (ie, the higher the temperature) required to convert it from a solid to a liquid state. The presence of oil inside the NLC system may assist in distributing the heat energy more homogeneously. Oils containing a high proportion of unsaturated fatty acids are generally liquid, and double bonds present in the carbon chain reduce the melting point. This may result in more efficient emulsification in NLC systems, which in turn has an effect on the size of the droplets formed. Upon cooling, pre-emulsion has smaller droplets, which may result in smaller nanoparticles. It was reported that the broader the spectrum of triglycerides present in the oil, the broader the melting range.[25]

DSC enables an insight into the melting and recrystallization behavior of crystalline materials, such as lipid nanoparticles. The breakdown of the crystal lattice by heating reveals further information on the polymorphism, crystal ordering, eutectic mixtures, and/or the glass transition process.[26] DSC experiments are useful to understand drug and lipid interactions and mixture behaviors such as C 888 and Miglyol. Therefore, DSC analysis was conducted to investigate the melting and crystallization behavior of both SLNs and NLCs. The thermograms of blank and loaded formulations are shown in Figures 1 and 2.

The melting process for C 888 and RSV took place with maximum peaks at 72.31°C and 265.83°C, respectively. It was observed that lipid C 888 was completely crystalline in SLN as seen in Figure 1. The RSV peak was lost in both SLN and NLC formulations, highlighting the solubilization of RSV in the lipid phase, as seen in Figure 2. The melting point of C 888 in NLC formulations was slightly lower. The polymorphism was also determined in prepared NLC formulations. In previous studies it was reported that adding Miglyol to the carrier depresses the melting point in a concentration-dependent manner.[27]

The ZP of blank NLC did not differ with the amount of oil used ($P > 0.05$). When RSV was loaded, the overall charge reduced as in the case of the SLNs. However, the lowest electrical charge (highest mV) was observed at an oil concentration of 15%. When the RSV-loading capacity was compared, the highest EE was obtained at the same concentration (RN2). Thus, it was concluded that encapsulation of RSV had an effect on the charge of the NLC system.

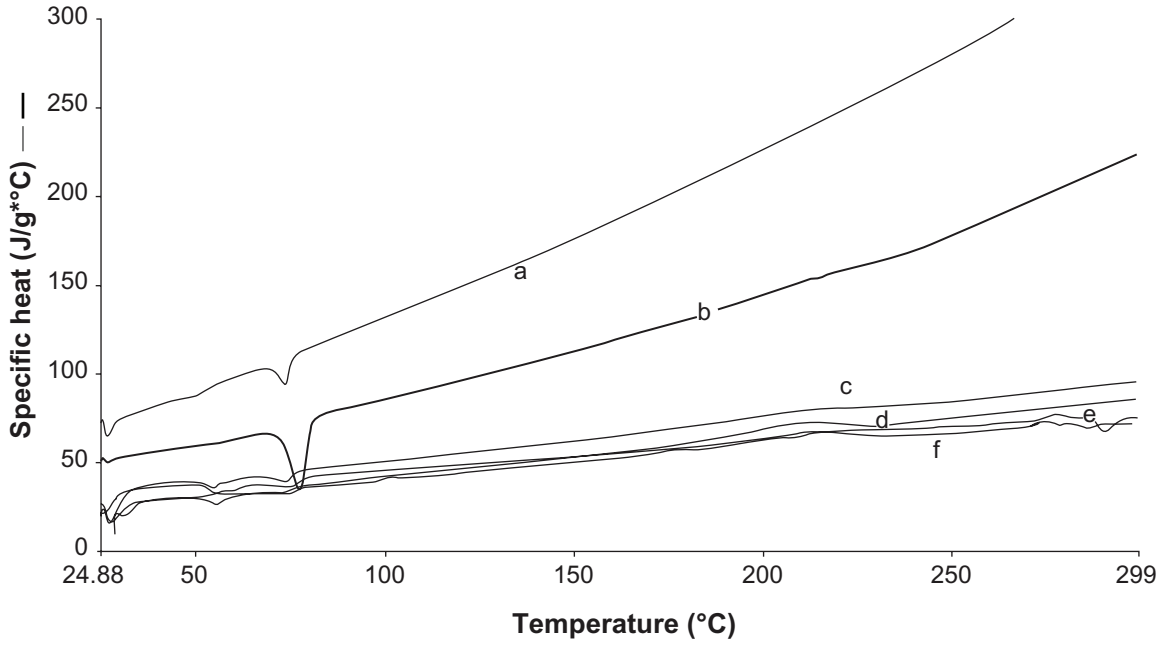

Figure 1 Differential scanning calorimetry thermograms of (**a**) blank solid lipid nanoparticles; S1 (**b**) bulk C 888 (**c**) N2 (**d**) N3 (**e**) N4 (**f**) N1.

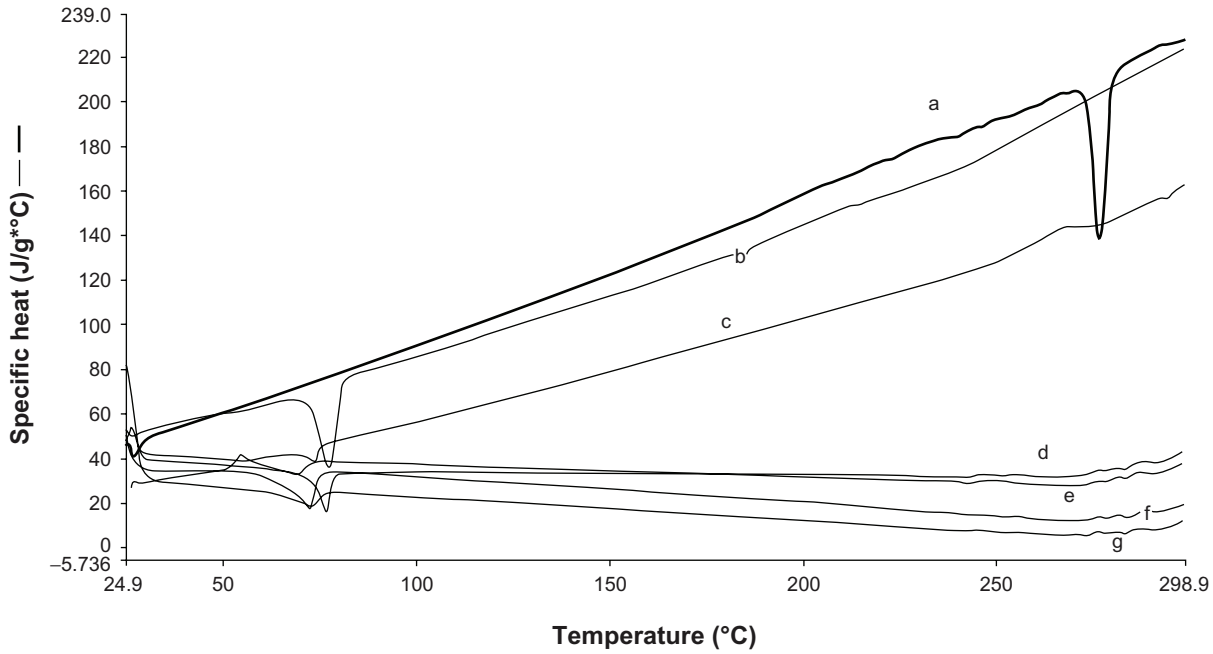

Figure 2 Differential scanning calorimetry thermograms of (**a**) resveratrol, (**b**) compritol, (**c**) RN1, (**d**) RN4, (**e**) RN2, (**f**) RS4, (**g**) RN3.

TEM analysis confirmed the colloidal sizes of loaded SLN and NLC seen in Figure 3. The regular round shapes of the nanoparticles had changed into more amorphous shapes, and crystallization of RSV on the surface of SLN could be observed in the images. The reason for the settlement of the drug on the surface of the solid lipid matrix – drug-enriched shell model – might be explained by the significant difference between the melting points of the lipid and the drug. The drug-enriched shell model is characterized by the drug located at the interface of the lipid and the surfactants, either by fast solidification of the lipid matrix, or by the successful competition of the drug for the interface due to solubility properties. According to this model of drug incorporation, a solid lipid core is formed when the recrystallization temperature of the lipid is reached.[17,28]

Table 3 PS, PI, and ZP of NLCs prepared

Code	PS (nm) ± SD	PI ± SD	ZP (mV) ± SD	EE%
N1	106.1 ± 1.64	0.292 ± 0.05	–21.7 ± 3.5	–
N2	108.1 ± 0.05	0.288 ± 0.05	–22.3 ± 1.1	–
N3	120.9 ± 0.5	0.241 ± 0.01	–24.3 ± 1.1	–
N4	136.3 ± 1.4	0.221 ± 0.01	–22.0 ± 2.2	–
RN1	90.58 ± 1.7	0.280 ± 0.06	–16.1 ± 0.1	82
RN2	110.5 ± 1.3	0.259 ± 0.01	–13.8 ± 0.1	91
RN3	117.3 ± 1.6	0.224 ± 0.03	–15.2 ± 0.6	72
RN4	148.7 ± 1.5	0.213 ± 0.01	–16.3 ± 0.08	78

Note: Data are presented as mean ± SD standard deviation (SD).
Abbreviations: EE, entrapment efficiency; PI, polydispersity index; PS, particle size; ZP, zeta potential; NLCs, nanostructured lipid carriers.

In our study, it was suggested that, once the lipid solidification was completed, RSV was pushed to the outside of the lipid matrix, without the possibility of being accomodated inside the crystallized lipid and instead locating in the outer shell. However, we did not observe the same images with NLC. Adding liquid oil not only enhanced the loading capacity, but may also have altered the model of drug loading. The lipid matrix of NLC was shown to solidify upon cooling, but it remained in the amorphous state.[17] This phenomenon may help in hosting RSV in a lipid matrix.

After determination of the optimum amounts of SLN (RS4) and NLC (RN2), cell culture studies were conducted to evaluate the effect of both the nanoparticle type and also the concentration of RSV on the fibroblast cell viability (see Figure 4).

Our cell culture studies revealed that at higher concentrations, a dramatic rate of cell death occurred. At the level of 250 μM, 40% of the cells were dead and at 500 μM, dramatic toxicity was observed ($P < 0.05$). Concentrations below 50 μM were determined as suitable RSV concentrations for both SLN and NLC, as seen in Figure 4. The concentrations of 10 μM, 25 μM, and 50 μM were found to be suitable RSV concentrations, given the percentage ratio of RSV to fibroblast cell vitality. The type of system (SLN or NLC) did not produce a significant difference in cell cytotoxicity. In a previous study, it was reported that the cells remained completely viable after exposure to SLN at an RSV concentration of 100 μM.[20] However, in our study, optimum RSV concentration was

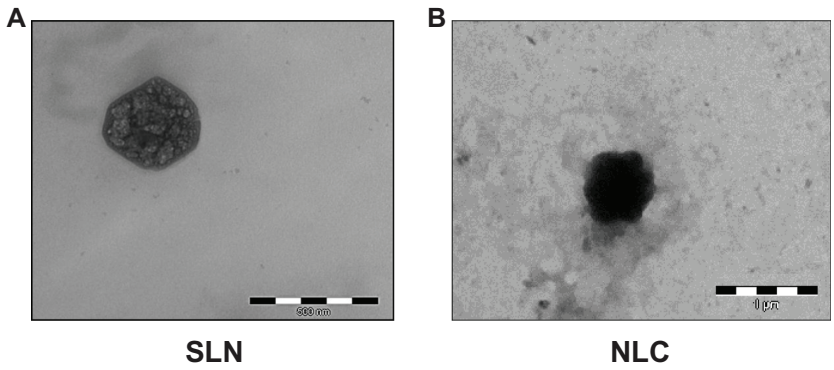

Figure 3 Transmission electron microscopy images of (**A**) resveratrol (RSV)-loaded solid lipid nanoparticles (SLN) (S4) (**B**) RSV-loaded nanostructured lipid carriers (NLC) (RN2).

determined to be 50 μM for both SLN and NLC, since the highest viability was obtained at this concentration.

Figure 5 represents the number of cells versus fluorimetric intensity. The peaks are the results of ROS produced inside the cells, and this production is expressed as additional fluorescence. Thus, the higher the fluorescence, the lower the antioxidant effect. The concentration of DCFH-DA was chosen as 1 mM in order to differentiate between ROS fluorescence and noise.

Figure 6 represents the histogram number of cells versus fluorimetric intensity evaluated for RSV, RSV-loaded SLN and NLC, control, and H_2O_2-treated samples.

Furthermore, the morphologic parameters of the cell substrates treated with SLN and NLC samples demonstrated that they were viable (Figure 7), indicating that the oxidative damage did not cause cell death. The fluorescence intensity is directly related to ROS production due to the oxidative damage caused by H_2O_2 treatment. The higher the fluorescence, the higher the concentration of intracellular ROS. The cell substrate treated with H_2O_2 showed the highest ROS accumulation, as indicated by the cell peak characterized by fluorescence intensity ranging from 10–100 au. The control cell substrate had the lowest ROS accumulation; all the cells counted presented a fluorescence intensity of below 10. The cell substrates treated with RSV alone or loaded in the colloidal systems had cell fluorescence intensities below that of the substrate treated with H_2O_2 alone.

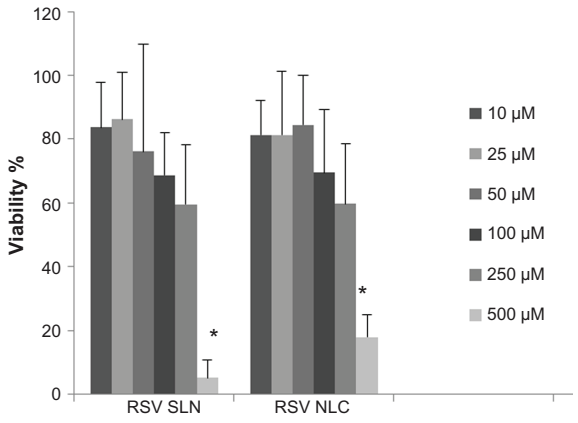

Figure 4 Viability % of fibroblast cells after 24 h treatment with 10, 25, 50, 100, 250 and 500 μM of solid lipid nanoparticles (SLN) and nanostructured lipid carriers (NLC).

Notes: The results are the means ± standard deviation. *$P < 0.05$; Viability % of fibroblasts determined after exposure to 500 μM of resveratrol (RSV) concentration in SLN or NLC vs all other RSV concentrations.

This indicates that the presence of RSV, either alone or loaded in the colloidal systems will decrease ROS accumulation and accordingly exert antioxidant activity. These results are in agreement with integration values of % fluorescence intensity vs cell counted curve calculated in the range of 10%–100% fluorescence intensity for the samples (Figure 7). RSV alone and both the RSV-loaded colloidal systems were characterized by a fluorescence intensity below that of the substrate treated with H_2O_2 alone ($P < 0.05$).

Generally, antioxidant molecules are inherently unstable in nature and are susceptible to photodegradation in the presence of oxygen, which makes them difficult to formulate into an acceptable, stable product for dermal application.[29] The stability of chemical labile hydrophobic antioxidants like retinol, Coenzyme Q10, alpha-lipoic acid, beta-carotene, and alpha-tocopherol could be enhanced when incorporating them into lipid nanoparticles.[30–32] Thus, the encapsulation of RSV into a lipid nanosystem might also be helpful in improving stability, whilst performing a protective effect as sufficiently as the RSV molecule itself.

The mean fluorescence intensity percentage results obtained from cytofluorimetry studies could be listed in order as: RSV $_{(31.17)}$ > RSV-SLN $_{(32.06)}$ > RSV-NLC $_{(30.69)}$ > Control $_{(28.77)}$. RSV-loaded NLC showed a percentage value of fluorescence below those of RSV and RSV-loaded SLN, indicating less ROS production, although this was not statistically significant. This result could be due to both PS and ZP, in that smaller dimensions of RSV-loaded NLC with a reduced negative electrical charge should favor NLC fibroblast

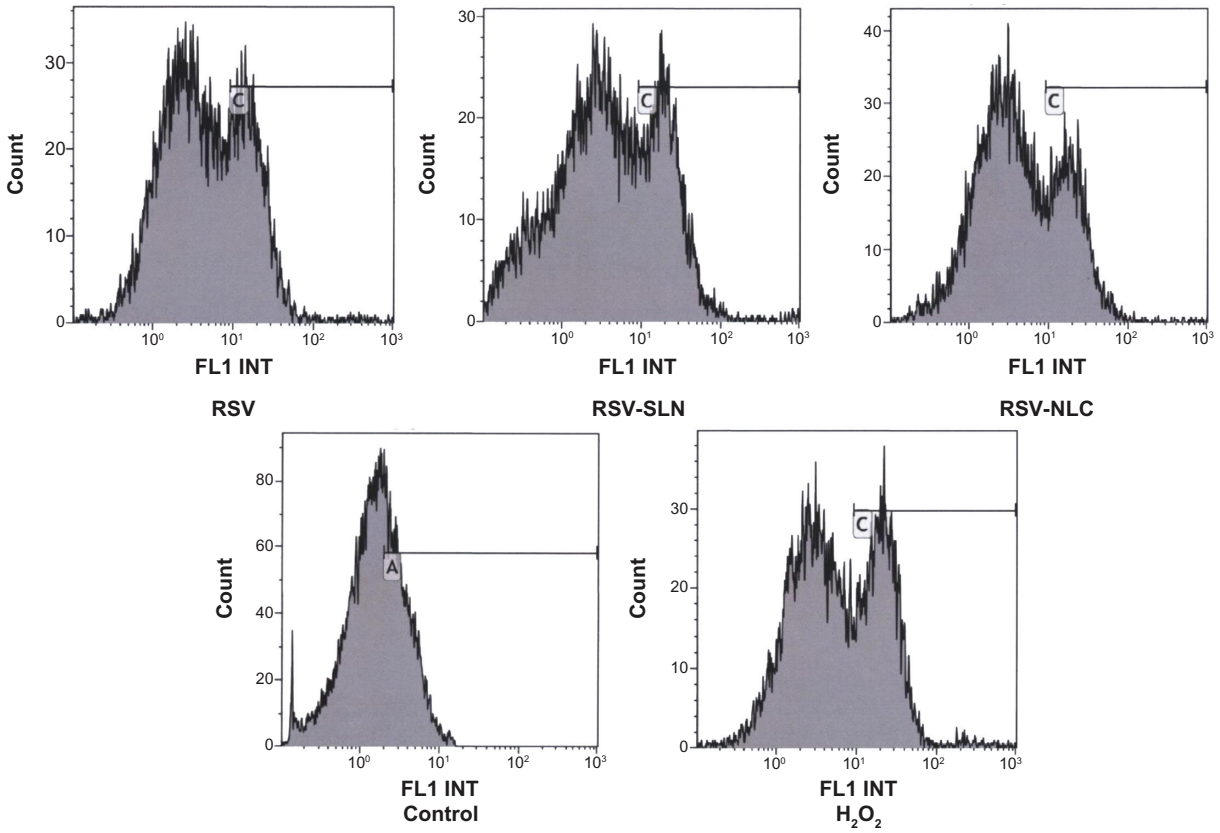

Figure 5 Signal intensity histograms of cells incubated with resveratrol (RSV), RSV-loaded solid lipid nanoparticles (SLN) (RS4) nanostructured lipid carriers (NLC) (RN2), control and H_2O_2-treated samples.

endocytosis. In fact, it is well known that reducing the anionic charge on nanoparticle carriers increases nonspecific interactions with cell surfaces.[33] This was also demonstrated in cytofluorometry studies by Hayes et al, where positively charged nanoparticles were shown to have a tendency to bind to cell surfaces and become endocytosed.[34]

Ex vivo skin diffusion studies were also conducted to analyze the diffusion and skin accumulation of RSV. Under the conditions of our study, after 24 hours, no RSV could be detected in the receptor phase (ethanol and water at a ratio of 1:1) with both SLN and NLC. Given that there was no transport of RSV into the receptor phase of Franz diffusion cells, it was thought that encapsulation of RSV into SLN or NLC might have improved the accumulation of RSV into the skin. Therefore, the skin samples were homogenized, and the accumulation of RSV was investigated (see Figure 8).

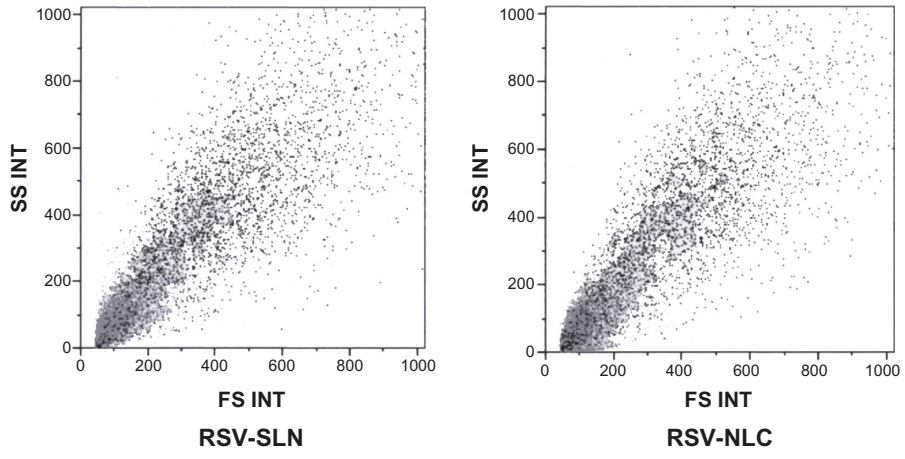

Figure 6 Morphologic parameter of fibroblasts treated with solid lipid nanoparticle (SLN) and nanostructured lipid carrier (NLC) samples.
Abbreviation: RSV, resveratrol.

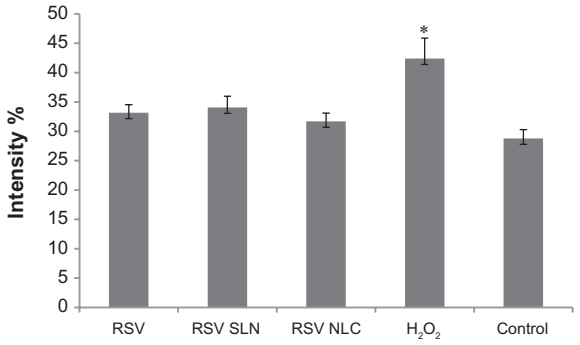

Figure 7 Integration of % fluorescence intensity vs cell counted curve in the range of 10–100 fluorescence intensity, obtained for cells incubated with resveratrol (RSV), RSV-loaded optimum solid lipid nanoparticles (SLN) and nanostructured lipid carriers (NLC) in comparison with control (positive) and H_2O_2 (negative).
Notes: *$P < 0.05$; fluorescence intensity % of H_2O_2 applied cells versus control, RSV, RSV-SLN, RSV-NLC applied groups.

RSV could be extracted from nanoparticle-treated skin samples (SLN: 1.55 ± 0.13 µg/cm^2, NLC: 1.99 ± 0.17 µg/cm^2). This phenomenon of RSV accumulation in the skin could be explained by the lipid characteristics of both the SLN and NLC systems, and in particular by the lipid-to-water partition coefficient of RSV. As observed in our previous study conducted with cyclosporine A incorporated SLNs, when the log P of the drug was high, enzymatic degradation (namely lipase degradation) should occur, and the drug would be released in situ.[21] Since the logP of RSV is approximately 3,[35] it was preferentially partitioned in the lipid phase of the nanoparticles, irrespective of the nanoparticle type.

However, the accumulation of RSV in both dermis and epidermis showed significant differences depending on nanoparticle type. Dermis accumulation was more significant for NLC; however, more epidermal accumulation was observed with SLN (see Figure 8). The difference between epidermis and dermis accumulation indicated that the most likely site of

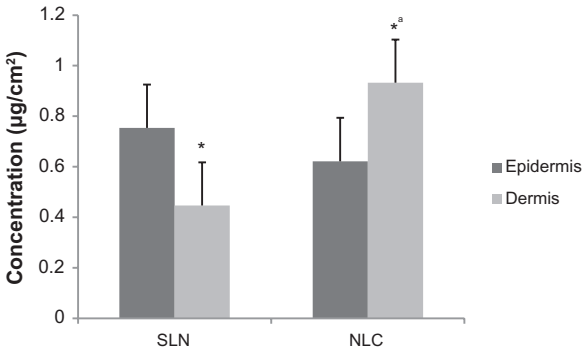

Figure 8 The amount of resveratrol (RSV) determined from the epidermis (dark bars) and dermis (light bars) of rat abdominal skin tissue.
Notes: *$P < 0.05$; RSV amount determined from dermis vs epidermis after exposure to both solid lipid nanoparticles (SLN) and nanostructured lipid carriers (NLC) systems, $^{a}P < 0.05$; RSV amount determined from RSV-loaded NLC applied epidermis vs RSV-loaded SLN applied epidermis.

accumulation might be the the appendages of the skin, such as hair and glands, where the nanostructure could enter until the complete degradation of the structure had occurred, as has previously been shown for lecithin/chitosan nanoparticles.[24] It was thought that smaller PS with the correspondingly reduced electrical charge helped the penetration of the NLCs to deeper layers of skin tissue.

Conclusion

RSV-loaded SLN and NLC have been prepared by means of the high shear homogenization method. Compritol C888 (for both SLN and NLC) and Miglyol 812 (for NLC alone) were used as the lipid phase. The optimal SLN and NLC formulations were based on a 60:1 lipid-to-drug ratio. In the NLC system, the optimal liquid lipid concentration was 15% of the whole lipid phase (Compritol and Miglyol).

Both RSV-loaded SLN and NLC systems were characterized by high biocompatibility, with normal human dermal fibroblasts at a concentration of 50 µM of RSV. At this concentration, RSV loaded in both the colloidal systems was effective in decreasing ROS accumulation exerting antioxidant activity.

Ex vivo skin diffusion studies showed that RSV was unable to permeate skin tissue. However, both systems permitted the penetration/accumulation of RSV into skin. NLC was characterized by better performance, indicating that NLC had a noticeably higher tendency to penetrate into skin with respect to SLN. In particular, NLC demonstrated better dermis accumulation, which could be determined by smaller PS and lower ZP, favoring particle penetration and possibly cell endocytosis.

The NLC formulation containing 255 mg of Compritol and 45 mg of Mygliol (15% of the lipid phase) was the most promising formulation. In particular, it demonstrated a fibroblast protection against intracellular ROS accumulation, and was suitable for the delivery of RSV, enhancing drug penetration/accumulation into the skin. Further studies will be undertaken to evaluate in vivo efficacy.

Acknowledgments

We wish to thank Dr G Viarengo and Dr M Cervio from the hospital IRCCS Policlinico San Matteo S.C. SIMT, at the Servizio di Immunoematologia e Medicina Trasfusionale for the measurements of cytofluorimetry. We wish to thank Novartis, Turkey, for financial support given for this study. We would also like to thank European Frame Socrates/Erasmus Program, for giving us the opportunity to exchange ideas and facilities in conducting this work.

Disclosure

The authors declare no conflicts of interest in this work.

References

1. Montesano-Gesualdi N, Chirico G, Catanese MT, Pirozzi G, Esposito F. AROS-29 is involved in adaptive response to oxidative stress. *Free Radic Res*. 2006;40(5):467–476.
2. Black HS, de Gruijl FR, Forbes PD, et al. Photocarcinogenesis: an overview. *J Photochem Photobiol B*. 1997;40(1):29–47.
3. Huei R, Neta P. Chemistry of reactive oxygen species. In: Gilbert DL, Colton CA, editors. *Reactive Oxygen Species in Biological Systems: An Interdisciplinary Approach*. New York: Springer; 2002: 33–73.
4. Portugal M, Barak V, Ginsburg I, Kohen R. Interplay among oxidants, antioxidants, and cytokines in skin disorders: present status and future considerations. *Biomed Pharmacother*. 2007;61(7):412–422.
5. Scharffetter-Kochanek K, Wlaschek M, Brenneisen P, Schauen M, Blaudschun R, Wenk J. UV-induced reactive oxygen species in photocarcinogenesis and photoaging. *Biol Chem*. 1997;378(11):1247–1257.
6. Trenam CW, Blake DR, Morris CJ. Skin inflammation: reactive oxygen species and the role of iron. *J Invest Dermatol*. 1992;99(6):675–682.
7. Afaq F, Adhami VM, Ahmad N. Prevention of short-term ultraviolet B radiation-mediated damages by resveratrol in SKH-1 hairless mice. *Toxicol Appl Pharmacol*. 2003;186(1):28–37.
8. van Ginkel PR, Sareen D, Subramanian L, et al. Resveratrol inhibits tumor growth of human neuroblastoma and mediates apoptosis by directly targeting mitochondria. *Clin Cancer Res*. 2007;13(17):5162–5169.
9. Mehnert W, Mäder K. Solid lipid nanoparticles: production, characterization and applications. *Adv Drug Deliv Rev*. 2001;47(2–3): 165–196.
10. Müller RH, Mäder K, Gohla S. Solid lipid nanoparticles (SLN) for controlled drug delivery – a review of the state of the art. *Eur J Pharm Biopharm*. 2000;50(1):161–177.
11. Jenning V, Gohla SH. Encapsulation of retinoids in solid lipid nanoparticles (SLN). *J Microencapsul*. 2001;18(2):149–158.
12. Wissing SA, Müller RH, Manthei L, Mayer C. Structural characterization of Q10-loaded solid lipid nanoparticles by NMR spectroscopy. *Pharm Res*. 2004;21(3):400–405.
13. Müller RH, Runge S, Ravelli V, Mehnert W, Thunemann AF, Souto EB. Oral bioavailability of cyclosporine: solid lipid nanoparticles (SLN) versus drug nanocrystals. *Int J Pharm*. 2006;317(1):82–89.
14. Küchler S, Wolf NB, Heilmann S, et al. 3D-wound healing model: influence of morphine and solid lipid nanoparticles. *J Biotechnol*. 2010;148(1):24–30.
15. Dingler A, Blum RP, Niehus H, Müller RH, Gohla S. Solid lipid nanoparticles (SLN/Lipopearls) – a pharmaceutical and cosmetic carrier for the application of vitamin E in dermal products. *J Microencapsul*. 1999;16(6):751–767.
16. Puglia C, Filosa R, Peduto A, et al. Evaluation of alternative strategies to optimize ketorolac transdermal delivery. *AAPS Pharm Sci Technol*. 2006;7(3):64.
17. Souto EB, Wissing SA, Barbosa CM, Müller RH. Development of a controlled release formulation based on SLN and NLC for topical clotrimazole delivery. *Int J Pharm*. 2004;278(1):71–77.
18. Teeranachaideekul V, Müller RH, Junyaprasert VB. Encapsulation of ascorbyl palmitate in nanostructured lipid carriers (NLC) – effects of formulation parameters on physicochemical stability. *Int J Pharm*. 2007;340(1–2):198–206.
19. Pardeike J, Hommoss A, Müller RH. Lipid nanoparticles (SLN, NLC) in cosmetic and pharmaceutical dermal products. *Int J Pharm*. 2009;366(1–2):170–184.
20. Teskac K, Kristl J. The evidence for solid lipid nanoparticles mediated cell uptake of resveratrol. *Int J Pharm*. 2010;390(1):61–69.
21. Gokce EH, Sandri G, Bonferoni MC, et al. Cyclosporine A loaded SLNs: evaluation of cellular uptake and corneal cytotoxicity. *Int J Pharm*. 2008;364(1):76–86.
22. Jang JH, Surh YJ. Protective effects of resveratrol on hydrogen peroxide-induced apoptosis in rat pheochromocytoma (PC12) cells. *Mutation Res*. 2001;496(1–2):181–190.
23. Afzal M, Matsugo B, Aoyama K, Takeuchi T. Method to overcome photoreaction, a serious drawback to the use of dichlorofluorescin in evaluation of reactive oxygen species. *Biochem Biophys Res Commun*. 2003;304(4):619–624.
24. Şenyiğit T, Sonvico F, Barbieri S, Özer Ö, Santi P, Colombo P. Lecithin/chitosan nanoparticles of clobetasol-17-propionate capable of accumulation in pig skin. *J Control Rel*. 2010;142(3):368–673.
25. Timms RE. Fractional crystallization – the fat modification process for the 21st century. *Eur J Lipid Sci Technol*. 2005;107:48–57.
26. Illingworth D. Fractionation of fats. In: Marangoni AG, Narine SS, editors. *Physical Properties of Lipids*. New York: Marcel Dekker, 2002;411–477.
27. Jenning V, Thünemann AF, Gohla SH. Characterisation of a novel solid lipid nanoparticle carrier system based on binary mixtures of liquid and solid lipids. *Int J Pharm*. 2000;199(2):167–177.
28. Uner M, Yener G. Importance of solid lipid nanoparticles (SLN) in various administration routes and future perspectives. *Int J Nanomedicine*. 2007;2(3):289–300
29. Kaur IP, Kapila M, Agrawal R. Role of novel delivery systems in developing topical antioxidants as therapeutics to combat photoageing. *Ageing Res Rev*. 2007;6(4):271–288.
30. Souto EB, Muller RH. Nanoparticulate drug delivery systems. *Informa Healthcare U S A, Inc*. 2007;166:213–234.
31. Trombino S, Cassano R, Muzzalupo R, Pingitore A, Cione E, Picci N. Stearyl ferulate-based solid lipid nanoparticles for the encapsulation and stabilization of beta-carotene and alfa-tocopherol. *Colloids Surf B Biointerfaces*. 2009;72(2):181–187.
32. Ruktanonchai U, Bejrapha P, Sakulkhu U, et al. Physicochemical characteristics, cytotoxicity, and antioxidant activity of three lipid nanoparticulate formulations of alpha-lipoic acid. *AAPS Pharm Sci Tech*. 2009;10(1):227–234.
33. Cullis PR, Chonn A, Semple SC. Interactions of liposomes and lipid-based carrier systems with blood proteins: relation to clearance behaviour in vivo. *Adv Drug Delivery Rev*. 1998;32(1–2):3–17.
34. Hayes ME, Drummond DC, Hong K, et al. Increased target specificity of anti-HER2 genospheres by modification of surface charge and degree of PEGylation. *Mol Pharm*. 2006;3(6):726–36.
35. Wesołowska O, Kuzdzał M, Strancar J, Michalak K. Interaction of the chemopreventive agent resveratrol and its metabolite, piceatannol, with model membranes. *Biochim Biophys Acta*. 2009;1788(9):1851–1860.